REGIONAL WATER TEMPERATURE CHARACTERISTICS OF LAKES SUBJECTED TO CLIMATE CHANGE

MIDHAT HONDZO and HEINZ G. STEFAN
University of Minnesota, Department of Civil and Mineral Engineering, St. Anthony Falls Hydraulic Laboratory, Minneapolis, Minnesota 55414, U.S.A.

Abstract. A deterministic, validated, one-dimensional, unsteady-state lake water quality model was linked to a daily weather data base to simulate daily water temperature profiles in lakes over a period of twenty-five (1955–79) years. Twenty seven classes of lakes which are characteristic for the north-central U.S. were investigated. Output from a global climate model (GISS) was used to modify the weather data base to account for a doubling of atmospheric CO_2. The simulations predict that, after climate change, epilimnetic temperatures will be higher but increase less than air temperature, hypolimnetic temperatures in seasonally stratified dimictic lakes will be largely unchanged or even lower than at present, evaporative water loss will be increased by as much as 300 mm for the season, onset of stratification will occur earlier and overturn later in the season, and overall lake stability will become greater in spring and summer.

1. Introduction

Freshwater lake temperatures respond to changed atmospheric conditions, and changes in lake water temperatures and temperature stratification dynamics may have a profound effect on lake ecosystems. Effects on fishes have been studied in particular by Coutant (1990), Magnuson *et al.* (1990) and Meisner *et al.* (1987). This paper deals with the question of how climate change may affect thermal aquatic habitat in lakes. A regional perspective is taken, and the scope is to estimate temperature changes in lakes of different morphometric and trophic characteristics in a region. Southern Minnesota is chosen as an example because an extensive lake database is available (ERLD/MNDNR, 1990). The geographic boundaries of Southern Minnesota are defined in Figure 1.

The response of lake water temperatures to climate changes can be investigated by several methods. One approach to finding climatic trends and their effect on lakes is to examine long-term records. In a few lakes, e.g. in the Experimental Lakes Area (ELA) in Ontario, Canada, or on Lake Mendota (Wisconsin) weekly and biweekly vertical profiles of water quality and biological parameters have been collected over periods of over several decades (Robertson, 1989; Schindler *et al.*, 1990). Observations indicate rising average surface water temperatures, and increased evaporation. Transparency and diversity in phytoplankton increased as well. Such trends can be determined only if lake temperature records are long enough. A second approach is to compare individual warm and cold, or wet and dry years if the records are short but detailed (Hondzo and Stefan, 1991). In order

Climatic Change **24**: 187–211, 1993.

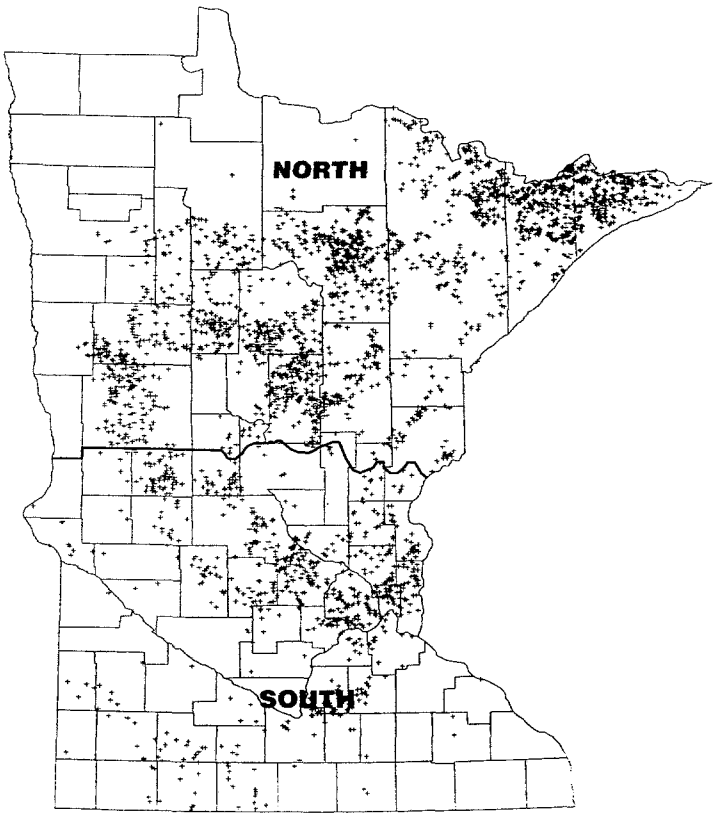

Fig. 1. Regional boundaries and geographic distribution of lakes in MLFD database.

extrapolate to lakes of different geometries and latitudes, and to possible future climates, a third approach using numerical simulation models is necessary. Such models calculate heat transfer from the atmosphere to the water and within the lake water column. Water temperature profiles in lakes are related to weather parameters by heat transport equations which apply basic conservation principles. This method allows linkage of various past and future climate scenarios to water temperatures in a physically meaningful way (McCormick, 1990; Schertzer and Sawchuk, 1990; Croley II, 1990; Blumberg and Di Toro, 1990).

Lake levels will be largely controlled by the water budget including evaporation and runoff. The response of watershed (surface) runoff to climate change is the subject of other investigations not included herein. Lake depths will therefore be treated herein as either invariant or will be lowered to account for increased evaporative water losses, where applicable. Changes in the watershed may affect nutrient loadings and hence primary productivity and transparency of the water. Such secondary effects also were not investigated, but a sensitivity analysis indicates that water temperature predictions for the types of lakes studied herein are usually only weakly sensitive to transparency. The probable reason is that the majority of these

lakes have strong light attenuation as indicated by surface mixed layer depths in excess of Secchi depths. Secchi depth is a frequently used visual measure of water column transparency. It is the depth at which a so-called Secchi disk disappears to an observer's eye when lowered into a column of water. Radiative heat input therefore heats the surface mixed layer regardless of where it is attenuated. Exceptions are shown for hypolimnetic water temperatures in Figure 6.

Herein a dynamic and validated lake water temperature model (Hondzo and Stefan, 1992b) will be applied to a representative range of lakes in a region for past climate and one future climate scenario. Rather than analyzing particular years and lakes, emphasis is on long term behavior and a wide range of lake morphometries and trophic levels. In this study the base period (or comparable reference) was from 1955–1979. For the same period of time weather parameters were perturbed by the $2 \times CO_2$ GISS (Goddard Institute for Space Studies) climate model output. The regional impact of these climates on different lake classes in southern Minnesota is reported herein. The simulated water temperatures, past and future, will be presented, interpreted and related to the lake characteristics and climate characteristics. The results will show how water temperatures in different freshwater lakes respond to changed atmospheric conditions in a region.

2. Method of Lake Temperature Modeling

In this study a one-dimensional lake water quality model, which has been previously successfully applied to simulate hydrothermal processes in different lakes and for a variety of meteorological conditions was used (Stefan and Ford, 1975; Ford and Stefan, 1980; Stefan *et al.*, 1980; Riley and Stefan, 1988; Gu and Stefan, 1990; Stefan, 1989; Hondzo and Stefan, 1991). In the model the lake is described by a system of well mixed horizontal layers. The model includes physically based relationships for heat exchange between water and atmosphere. The model determines surface heat exchange rates by short-wave and long-wave radiation, back radiation, evaporation and convection/conduction. The total net heat loss or gain by the water is distributed throughout the water column by turbulent mixing and natural convection. Surface (epilimnion) heat transport is described by a wind mixing algorithm (Stefan and Ford, 1975). Hypolimnetic mixing is related to a diffusion coefficient which is related to lake morphometry and stratification stability (Hondzo and Stefan, 1992b).

The numerical model is applied in daily timesteps by using mean daily values for the meteorological variables. The required weather parameters are solar radiation, air temperature, dew point temperature, wind speed, wind direction, and precipitation. Initial conditions, lake morphometry (area-depth-volume), and Secchi depth have to be provided to use the model. Simulations were made from spring overturn to fall overturn. Since the date of spring overturn is unknown, the initial conditions were set at 4 °C on March 1 and reset at 4 °C on each following day until the simulation predicted a rising surface water temperature. In this manner the model found

its own end of spring overturn. March 1 was chosen as a starting date because it is 35 to 45 days before 'ice-out' under present climate conditions and 'ice-out' will advance no more than 30 days under the future $2 \times CO_2$ climate scenario (Robertson, 1989). Using this method there is no annual carryover of heat stored in the lakes during the winter. It is certain that lakes in the region studied will continue to remain dimictic (fall and spring turnover events at 4 °C) and will continue to have a winter ice-cover, except for a shorter period. The summer predictions are thus made quasi-independent of initial conditions and match measurements well (Hondzo and Stefan, 1991). The model is one-dimensional in depth and unsteady, i.e. it simulates water temperature distributions over depth in response to time variable weather. Vertical water temperature simulations are made over an entire season (March 1 to November 30) and in time steps of one day. The calculated daily water temperature profiles are analyzed statistically and presented graphically.

For the regional analysis the number of calibration coefficients in the model was reduced from the original four to zero (Hondzo and Stefan, 1992b). This was accomplished by introducing new (empirical) relationships which contain only measurable parameters. Maximum vertical turbulent thermal diffusivity in the hypolimnion was related to surface area and density gradients, wind sheltering was related to surface area, radiation attenuation was related to Secchi depth.

These relationships were derived from either additional field measurements or by simulation and calibration of lakes with extensive measured water temperature profiles, e.g. the functional relationship for the solar radiation attenuation versus Secchi depth is obtained from the measurements in 50 lakes in Minnesota.

The water temperature simulation model was validated against data from nine Minnesota lakes for several years (Hondzo and Stefan, 1992b). The model simulates onset of stratification, mixed layer depth, and water temperature well. Standard error between measurements and simulations was from 1.0 °C to 1.5 °C. The error is mostly associated with small differences between predicted and measured thermocline depths. Eight examples of measured and calculated water temperature profiles in Lake Calhoun throughout a season are shown in Figure 2. This lake falls into the category of deep (maximum depth larger than 20 m), medium area (0.4 to 5 km^2), and eutrophic (Secchi depth less than 1.8 m) lakes. Comparison shows that the onset of stratification, mixed layer depths, and temperatures were reasonably well predicted. Standard error was 1.0 °C.

3. Climate Conditions Simulated

Meteorological data from the Minneapolis-St. Paul International Airport (93.13° longitude, 44.53° latitude) were used. The meteorological data file assembled contains measured daily values of average air temperature, dew point temperature, precipitation, wind speed, and solar radiation from 1955 to 1979 (March–November). The period from 1955 to '79 was chosen because it is long enough to give a

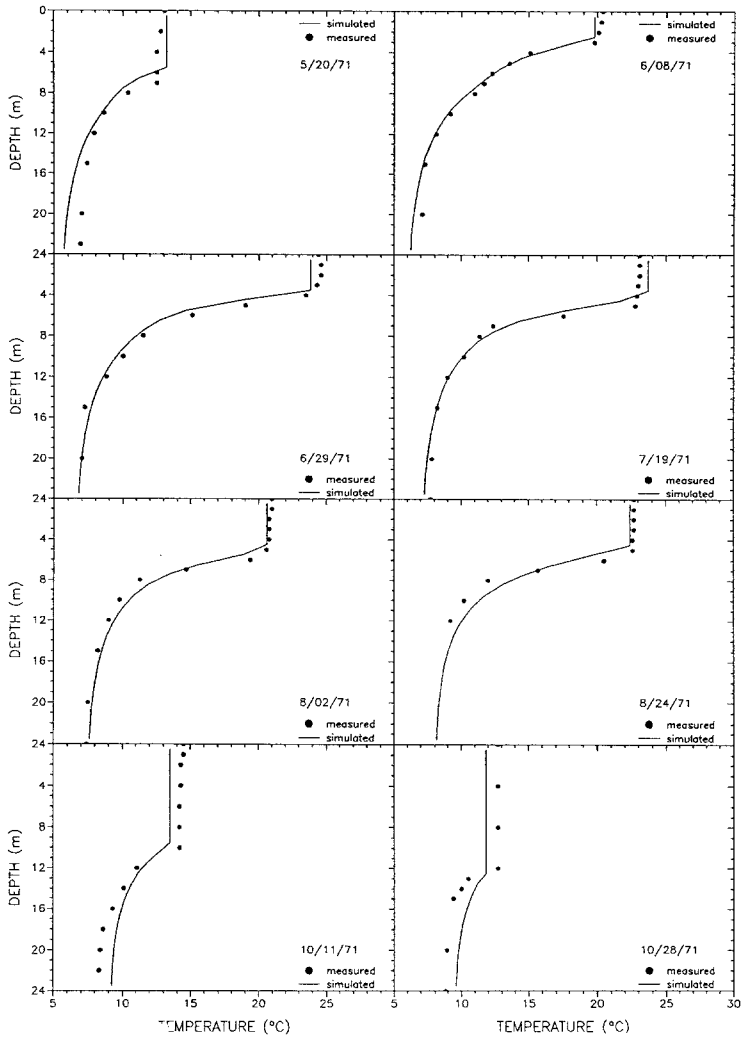

Fig. 2. Lake Calhoun water temperature profiles in 1971.

representative average of base conditions before climate warming. In the 1980s warmer than average air temperatures were observed (Jones *et al.*, 1986; Kerr, 1989), and therefore this period is excluded. Sources of climate data were as follows.

Climate scenarios were selected following EPA guidelines on global climate change effect studies (Robinson and Finkelstein, 1990). Climate projections by four different models (GISS, GFDL, OSU, UKMO) for the doubling of atmospheric CO_2 were provided by NOAA (1990). The models were developed at Columbia University's Goddard Institute for Space Studies (GISS), Princeton University's Geophysical Fluid Dynamics Laboratory (GFDL), Oregon State Univer-

sity (OSU), and the United Kingdom Meteorological Office (UKMO). The monthly climate projections by the four models are different from each other and their explicit effects on water temperature dynamics can be studied for each model separately. In this study only the GISS projections for the grid point closest to Minneapolis/St. Paul were used (Table I), as suggested by EPA for effect studies. A comparison of the mean monthly weather parameter values (for Minneapolis/St. Paul) projected by the four models shows that the GISS projections are not substantially different from GFDL and OSU, except for wind speeds in November. No adjustments were made to those wind speeds, however, for a lack of a rational basis and because late fall winds do not affect the summer water temperature dynamics. No interpolations between grid points were made, following explicit EPA recommendations (Robinson and Finkelstein, 1990).

The uncertainty of the climate predictions is not the subject of this paper. It is understood that relative humidity and wind speeds are not well predicted at the local scale by global climate models. Fortunately, uncertainty analysis of the effects of variable meteorological forcing on lake temperature models indicates that air temperature has the most significant effect in lake temperature uncertainty (Henderson-Sellers, 1988; Hondzo and Stefan, 1992a), and that parameter is better predicted than others.

Seasonal distributions of the 25-year average of observed weather parameters (which were used as model inputs) are shown in Figure 3. Past Climate and the $2 \times CO_2$ GISS scenario were used as inputs to the water temperature simulations.

TABLE I: Weather parameters changes projected by the $2 \times CO_2$ climate model output for Minneapolis/St. Paul

MAR	AIR TEMP. (diff. °C)	SOL. RAD. (ratio)‡	WIND S. (ratio)‡	REAL. HUM. (ratio)‡	PRECIP. (ratio)‡
JAN	6.20	0.92	0.92	1.16	1.17
FEB	5.50	1.04	1.12	1.01	1.03
MAR	5.20	0.98	0.47	1.13	1.28
APR	5.05	1.03	0.69	1.00	1.03
MAY	2.63	1.00	0.67	1.09	1.12
JUN	3.71	0.99	0.85	1.01	1.08
JUL	2.15	0.98	0.93	0.93	1.10
AUG	3.79	1.04	1.00	1.02	0.98
SEP	7.02	1.04	1.07	0.90	0.70
OCT	3.73	1.12	2.23	0.95	0.88
NOV	6.14	1.03	5.00	1.00	0.99
DEC	5.85	0.99	0.77	0.98	1.24

* Difference = $2 \times CO_2$ GISS − PAST.
‡ Ratio = $2 \times CO_2$ GISS/PAST.

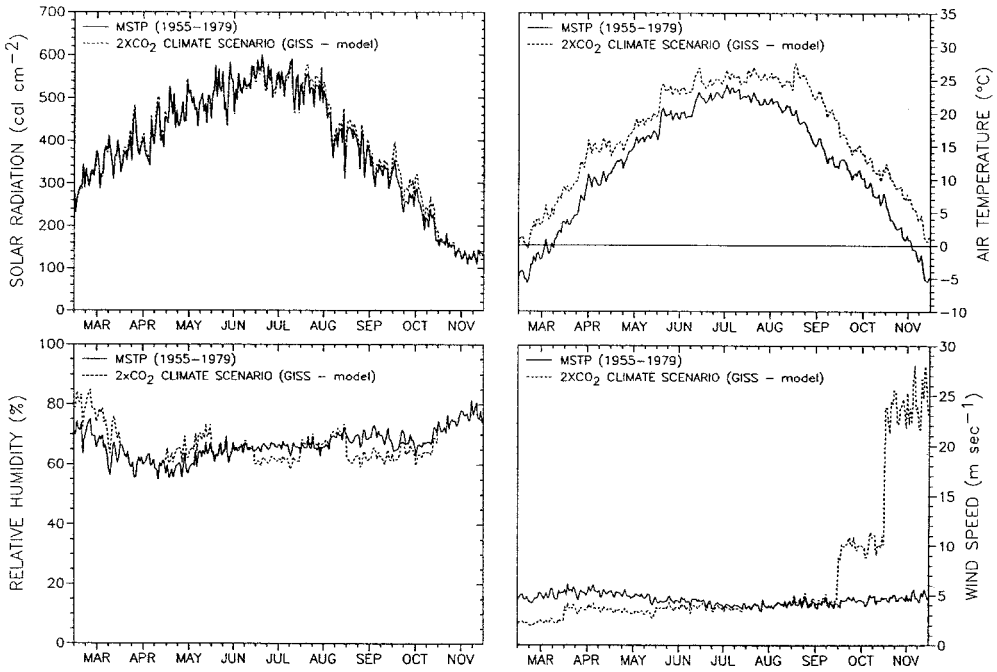

Fig. 3. Climate parameters at Minneapolis/St. Paul in the past and under a $2 \times CO_2$ (GISS) climate scenario.

4. Regional Lake Characteristics

Regional classification of lakes was approached in a variety of ways. The ecoregion approach (Omernick, 1987) was considered first, but found to give too detailed a picture. Ecoregion is defined as a region with homogeneous topographic, geologic, vegetative and land use features. The entire state was considered as a regional entity but rejected as too large because of the diversity of climate. Dividing the state into a northern and southern region was considered appropriate and not as arbitrary as might seem because there is a significant gradient in geological, topographic, hydrological, climatological, and ecological parameters across the mid-section of the state (Baker *et al.*, 1985, Heiskary *et al.*, 1987). The southern and northern regions are about equal in size (Figure 1).

The Minnesota Lakes Fisheries Database, MLFD (ERLD/MNDNR, 1990), contains lake survey data for 3002 Minnesota lakes. The MLFD database includes 22 physical variables and fish species. Nine primary variables explain 80% of the variability between lakes. These nine variables include surface area, volume, maximum depth, alkalinity, Secchi depth, lake shape, shoreline complexity, percent littoral area, and length of growing season. For regional classification of the lakes in

this study, the possible thermal structure (i.e. whether lakes are stratified or not) and trophic status are of primary concern. Observations in the northern hemisphere show that onset and maintenance of stratification in lakes is dependent on surface area and maximum depth (Gorham and Boyce, 1989) as well as on climatological forcing, i.e. solar radiation and wind (Ford and Stefan, 1980). Lake trophic status contributes to solar radiation attenuation and oxygen balance. Trophic status was assessed by using a Secchi depth scale (Heiskary and Wilson, 1988) related to Carlson's Trophic State Index (Carlson, 1977). Secchi depth information was available in the MLFD.

A statistical analysis of southern and northern Minnesota Lakes in the MLFD in terms of surface area, maximum depth and Secchi depth was made. The geographic distribution of different classes of lakes in Minnesota is given in Figure 4. Cumulative frequency distributions shown in Figure 5 were used to subdivide all lakes into three ranges of surface area, maximum depth and Secchi depth, as shown in Table II. These represent 27 classes of lakes in each of the two regions of the state. A representative value for surface area, maximum depth and Secchi depth was chosen in each lake class as input to the model simulation. Those values are shown under the heading 'class' in Table II.

Representative area-depth relationships for three different lake classes (by surface area) were obtained from 35 lakes which covered the entire range of distributions in a set of 122 lakes. After areas are expressed as fractions of surface area and depths are expressed as fractions of maximum depth, an equation of the form

$$Area = a \cdot \exp(b \cdot Depth) + c \tag{1}$$

is fitted to the data and subsequently used in the simulation as a representative area-depth relationship. Coefficients a, b, c, estimated by regression analysis are given in Table III. This procedure is equivalent to self-similarity of depth-area relationships within a given class.

TABLE II: Lake classification

Lake key parameter	Description	Class value	Range	Cumulative frequency
Area (km^2)	small	0.2	<0.4	lower 30%
	medium	1.7	0.4–5.0	central 60%
	large	10.0	>5.0	upper 10%
Maximum depth (m)	shallow	4.0	<6.0	lower 30%
	medium	13.0	6.0–20.0	central 60%
	deep	24.0	>20.0	upper 10%
Secchi depth (m)	eutrophic	1.2	<1.8	lower 30%
	mesotrophic	2.5	1.8–4.5	central 60%
	oligotrophic	4.5	>4.5	upper 10%

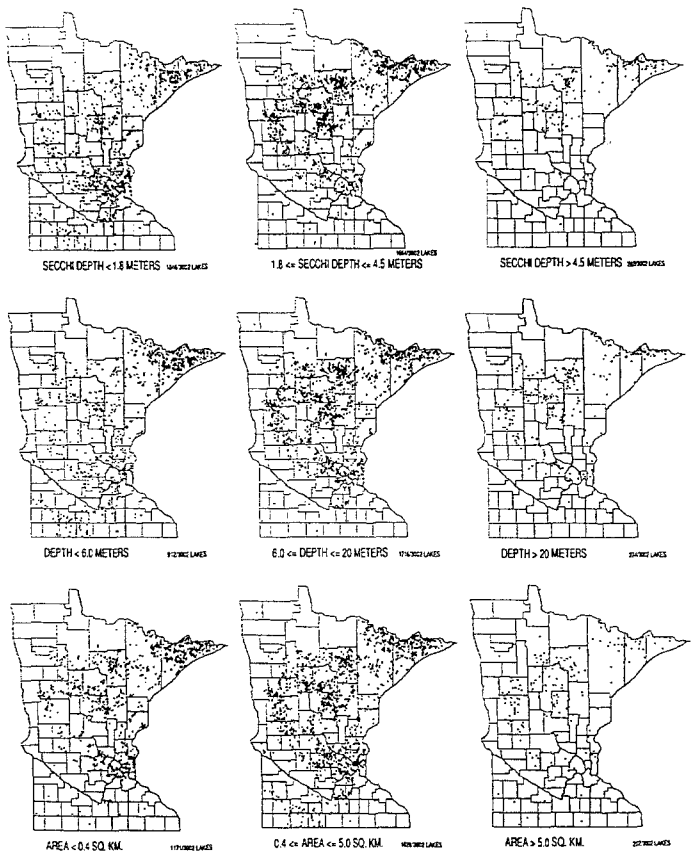

Fig. 4. Geographic distribution of lakes according to key parameters: Secchi depth, maximum depth, and surface area.

TABLE III: Morphometric regression coefficients a, b and c in the area vs. depth

Area	a	b	c	r^2
Small	1.19	−1.76	−0.20	0.90
Medium	1.14	−2.10	−0.15	0.92
Large	1.14	−2.91	−0.08	0.85

r^2 – portion of the measured lake area variability explained by the regression equation.

Lake basin shape was assumed circular for the purpose of wind fetch calculation. The water temperature simulation results were shown to be insensitive to these assumptions of morphometric self-similarity and basin shape.

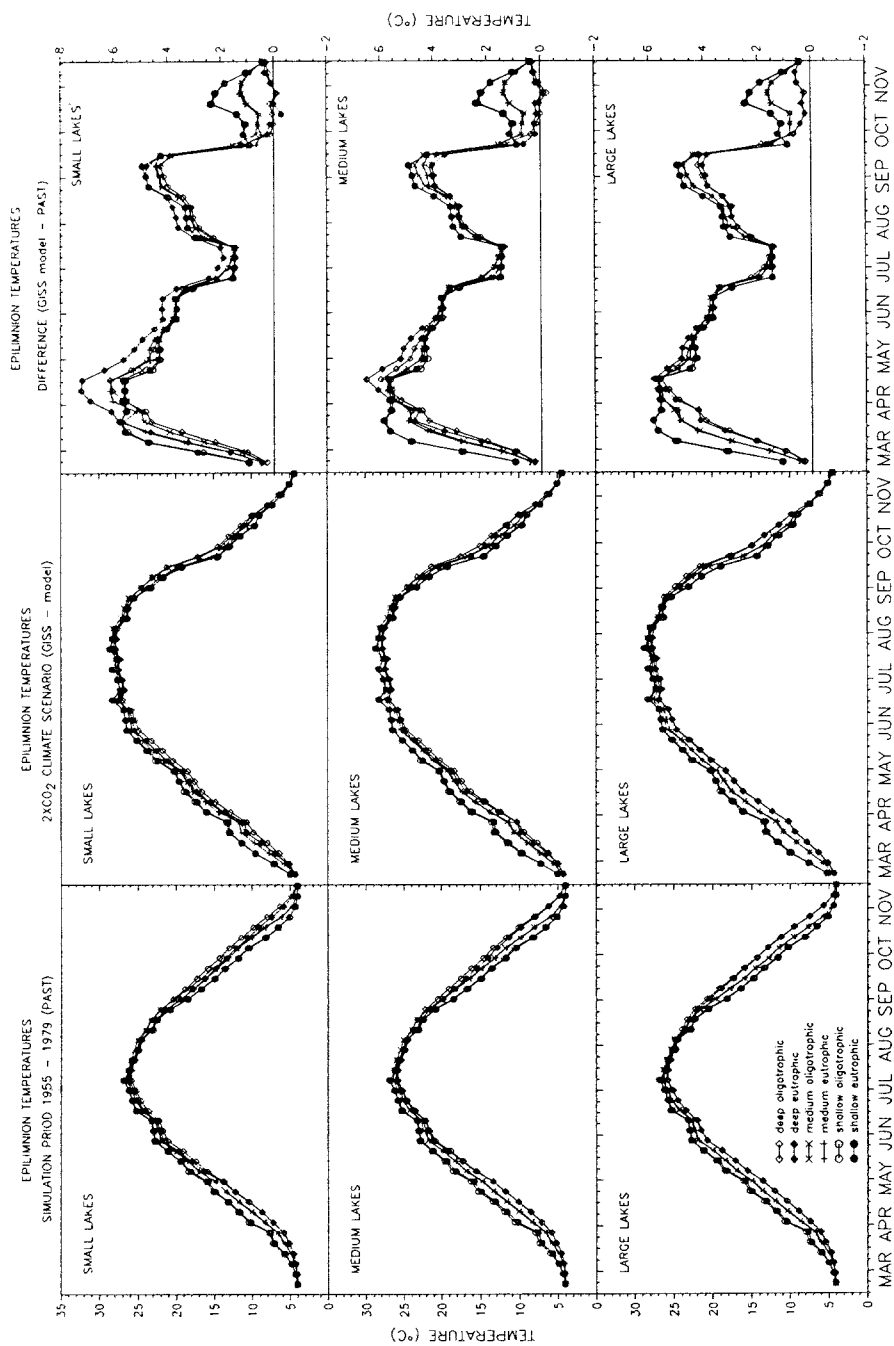

Fig. 5. Simulated weekly epilimnion temperatures.

5. Simulated Lake Water Temperature Regimes for Historical and Future Weather

5.1. *Water Temperatures*

Simulations of daily water temperature profiles from March 1 to November 30 (275 days) in each year from 1955 to 1979 (25 yr) were made for each of the 27 lake classes. In addition to lake morphometric input, i.e. surface area, maximum depth and depth-area relationship, these simulations used actually recorded daily values of weather parameters, i.e. solar radiation, air temperature, dew point temperature, wind speed, and precipitation for each day simulated. A massive weather-database had to be developed prior to the simulations. The calculated output of 185,625 vertical water temperature profiles, each consisting of 24 water temperature values, provided base line infomation on lake characteristics during a period of the past when little climate change occurred.

To simulate possible future water temperature regimes, the monthly corrections specified by the $2 \times CO_2$ GISS model scenario were applied to the weather data base and the simulations were repeated.

From these simulated water temperature data bases under historical and future climates, each consisting of 4,455,000 water temperature values, the following characteristics were extracted.

Epilimnetic water temperatures were defined as water temperatures at 1.0 m below the water surface regardless whether maximum-depth is 4 m, 13 m or 24 m, respectively. The seasonal course of epilimnetic temperatures, averaged weekly over 25 yr is shown in Figure 5 for both past climate and the $2 \times CO_2$ GISS climate scenario. The difference between the two is also shown in Figure 5; the associated air temperature increments due to climate change were presented in Table I. The largest weekly water temperature change in response to climate change is on the order of 6 to 7 °C, and occurs in spring (April), the minimum is on the order of 0 to 2 °C and occurs either in fall (October and November), or in July.

The GISS scenario gives a seasonal surface water temperature pattern different from that for the past. The cooling phase, for example, commences later and has stronger water temperature gradients. Maximum weekly surface water temperatures and the time of their occurrence are given in Table IV. The highest surface water temperatures, 27.4 °C (± 0.1 °C) were calculated for the shallow lakes and the lowest, 26.2 °C (± 0.1 °C) for the deep lakes. With climate change the predicted rise in the seasonal surface water temperature maxima is 1.9 to 2.2 °C, which is small compared to air temperature changes in Table I. The occurrence of the maximum water surface temperatures is shifted by 11 to 20 days towards the fall with the climate change.

Surface water temperatures are fairly independent of lake morphometry within the range of lakes investigated. Extreme values in lakes of different geometry vary by no more than 4 °C on any given day. Maximum differentials occur in spring and fall. From June through September, i.e. during the period of seasonal water tem-

TABLE IV: Maximum temperatures of Southern Minnesota lakes

			Past 1955–1979				GISS − 2 × CO_2				Difference (GISS − PAST)	
Maximum depth (m)	Area (km^2)	Trophic level	Epilimnion °C	day*	Hypolimnion °C	day*	Epilimnion °C	day*	Hypolimnion °C	day*	Epilimnion °C	Hypolimnion °C
Shallow (4.0)	Small (0.2)	eutrophic	27.5	203	24.9	206	29.4	217	26.2	229	1.9	1.3
		mesotrophic	27.4	203	26.8	204	29.4	217	28.3	218	2.0	1.5
		oligotrophic	27.3	203	27.0	203	29.3	217	29.2	217	2.0	2.2
	Medium (1.70)	eutrophic	27.4	203	26.2	204	29.4	217	27.5	205	2.0	1.3
		mesotrophic	27.4	203	27.0	203	29.5	217	29.1	181	2.1	2.1
		oligotrophic	27.3	203	27.1	203	29.4	217	29.4	217	2.1	2.3
	Large (10.0)	eutrophic	27.4	203	26.5	203	29.5	217	28.3	181	2.1	1.8
		mesotrophic	27.4	203	26.9	203	29.6	217	29.1	181	2.2	2.2
		oligotrophic	27.3	203	27.1	203	29.5	217	29.4	217	2.2	2.3
Medium (13.0)	Small (0.2)	eutrophic	26.6	203	11.9	278	28.7	217	12.6	289	2.1	0.7
		mesotrophic	26.5	206	12.8	277	28.7	218	13.0	284	2.2	0.2
		oligotrophic	26.6	203	17.5	261	28.7	218	17.5	276	2.1	0.0
	Medium (1.70)	eutrophic	26.4	204	18.7	254	28.5	218	18.2	274	2.1	−0.5
		mesotrophic	26.4	207	19.9	252	28.6	218	20.3	271	2.2	0.4
		oligotrophic	26.5	207	23.0	233	28.7	218	25.3	248	2.2	2.3
	Large (10.0)	eutrophic	26.5	203	24.0	220	28.6	223	26.0	233	2.1	2.0
		mesotrophic	26.5	206	24.6	218	28.7	218	26.6	224	2.2	2.0
		oligotrophic	26.6	207	25.5	211	28.7	218	27.3	218	2.1	1.8
Deep (24.0)	Small (0.2)	eutrophic	26.4	206	7.3	308	28.5	217	10.3	305	2.1	3.0
		mesotrophic	26.3	204	7.4	308	28.3	218	10.4	305	2.0	3.0
		oligotrophic	26.1	207	7.8	308	28.10	220	10.6	305	2.0	2.8
	Medium (1.70)	eutrophic	26.2	206	11.6	294	28.2	218	12.8	291	2.0	1.2
		mesotrophic	26.2	206	11.8	293	28.1	223	12.9	291	1.9	1.1
		oligotrophic	26.1	206	12.6	291	28.1	223	13.3	291	2.0	0.7
	Large (10.0)	eutrophic	26.1	206	18.2	261	28.1	223	18.4	276	2.0	0.2
		mesotrophic	26.1	206	18.4	263	28.1	223	18.7	276	2.0	0.3
		oligotrophic	26.1	207	19.4	259	28.2	218	20.1	273	2.1	0.7

* day = Julian day when maximum temperatures occur.

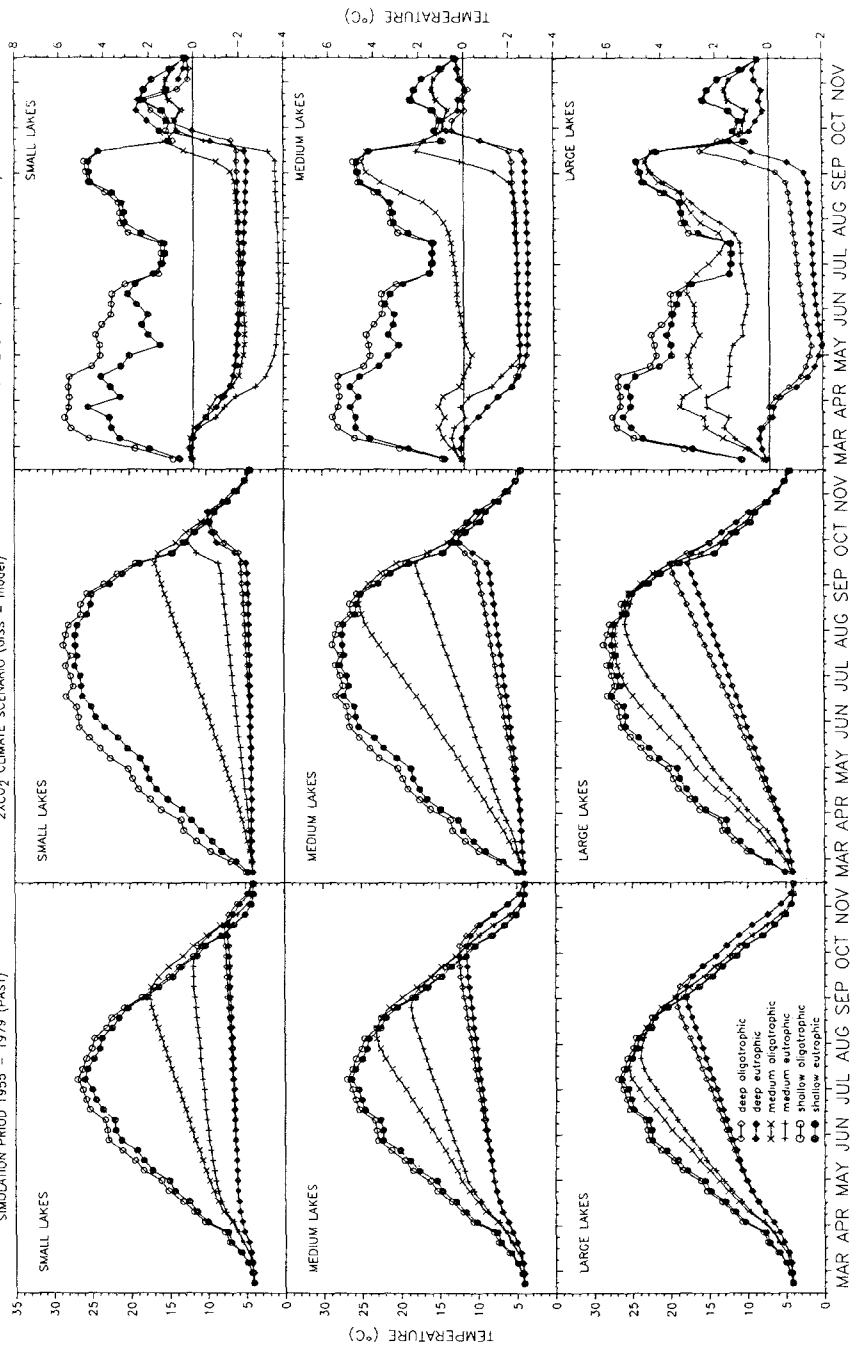

Fig. 6. Simulated weekly hypolimnion temperatures.

perature stratification, surface water temperatures in lakes of different morphometric characteristics (depth and area) are very similar (within 1.0 °C). In very large lakes (e.g. the North American Great Lakes) the significantly greater water volumes and mixed layer depths cause a substantial lag in heating and cooling leading to water temperature differences larger than 4 °C.

Weekly averages of 25 yr of simulated hypolimnetic temperatures are shown in Figure 6. Values are 1 m above the late bottom (maximum depth). Hypolimnetic temperature responses to climate change show wider variability than epilimnetic responses. In shallow (polymictic) lakes, the hypolimnetic and epilimnetic water temperature rise is very similar in magnitude and time of occurrence. In deep small lakes hypolimnetic temperatures are as much as 3.5 °C colder after climate change than before. The main reason for these surprising results is a more rapid onset of stratification early in spring due to an increased net rate of surface heating after climate change. The colder hypolimnetic water is thereby more quickly and effectively shielded from surface heating. Hypolimnetic warming during the summer is dependent on vertical turbulent diffusion and therefore wind fetch and hence surface area. Dependence of hypolimnetic temperatures on lake morphometry is very evident in Figure 6. The seasonal pattern of hypolimnetic water temperatures was altered by climate change most significantly in shallow lakes. All others showed typical seasonal warming patterns in response to vertical diffusion.

The highest hypolimnetic water temperatures (27.1 °C) were calculated for shallow oligotrophic lakes which are typically polymictic or well-mixed for the entire simulation period. The lowest maximum hypolimnetic temperatures (7.3 °C) occurred in small and deep eutrophic lakes. Climate change raised by 0 to 3 °C the maximum hypolimnetic water temperature or lowered it by as much as 3.5 °C, depending on the particular stratification dynamics of a lake.

In addition to long-term changes of water temperatures (Figures 5 and 6) variations from year to year are also of interest. Unfortunately weather parameters for the GISS climate scenario were only given as long term monthly averages. Therefore variability on an annual basis could not be explored for the GISS scenario. On the other hand, annual weather information was available for the 1955–79 period, and therefore could be used to give the range of simulated daily water temperatures. Bands of water temperatures within the 95% confidence interval are shown in Figure 7. The spread is significant and on the order of ± 3 to 5 °C around the mean, not only for surface temperature but also for hypolimnetic temperatures. This range is about twice as wide as that due to differences in lake morphometry (Figures 5 and 6). This is in agreement with field measurements by Ford and Stefan (1980) and has some bearing on habitat. Examples of water temperature structures in typical lakes are given in Figure 8.

5.2. *Thermal Energy Fluxes*

The water temperatures discussed above are, of course, the result of net heat

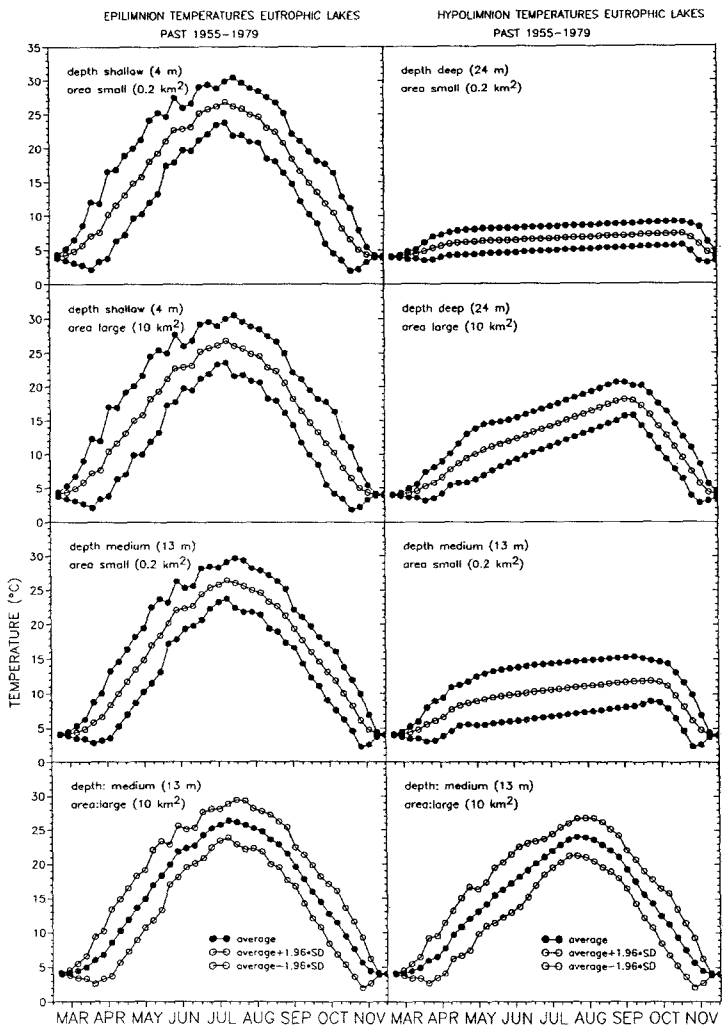

Fig. 7. Examples giving range of epilimnetic and hypolimnetic temperatures over a 25 yr period (95% confidence interval).

energy input or losses through the water surface, and vertical distributions of that heat within the lake. For better understanding of the water temperatures, it is therefore appropriate to consider, at least briefly heat fluxes and stratification dynamics. Five heat transfer processes are reponsible for heat input into the water: short wave solar radiation, long wave atmospheric radiation, conductive heat transfer, evaporation, and back radiation. Short wave solar radiation and atmospheric radiation increase the water temperature, while evaporation and back radiation cool the water. Conductive heat transfer can either heat or cool the water. All five fluxes together comprise net heat flux at the water surface. Individual daily heat fluxes vary dramatically with weather as is illustrated in Figure 9. To keep track of the

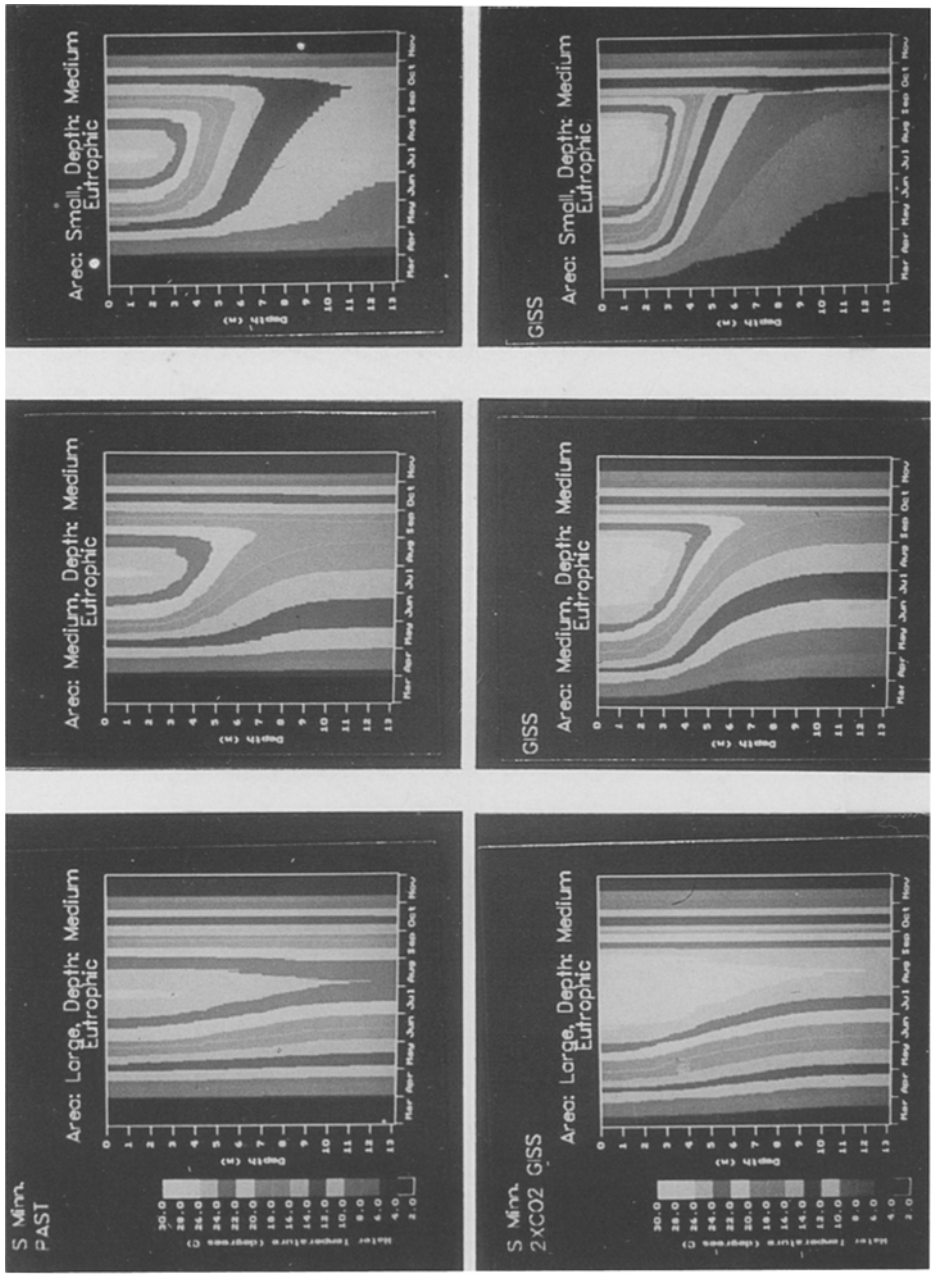

Fig. 8a. Simulated temperature (isotherm) structure in three medium deep (13 m maximum depth) lakes of large (10 km^2), medium (1.7 km^2) and small (0.2 km^2) surface area. Isotherm bands are in increments of 2 °C. Simulated water temperatures are for past climate (1955–79) (top) and the $2 \times CO_2$ GISS climate scenario (bottom).

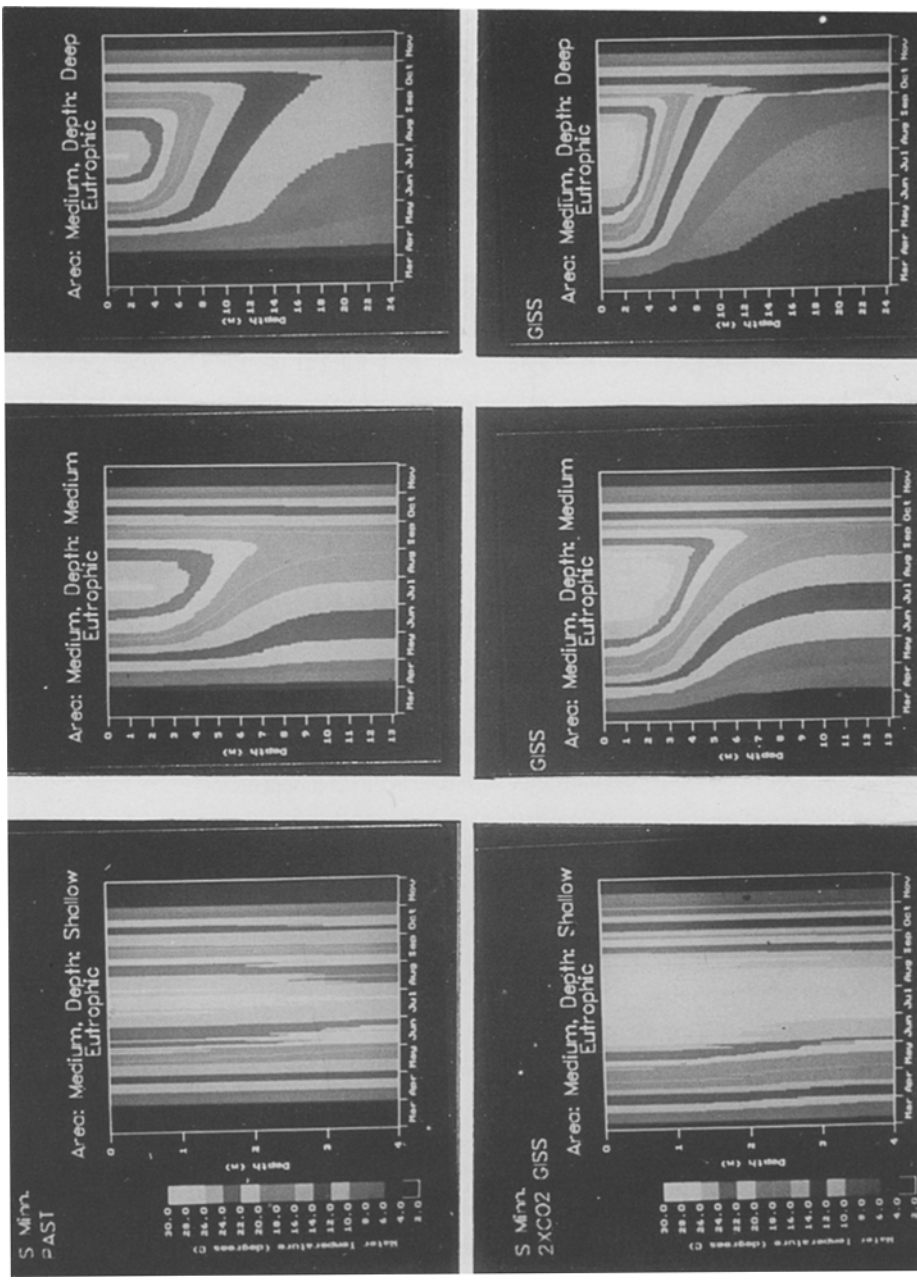

Fig. 8b. Simulated temperature (isotherm) structure in three medium area (1.7 km^2) lakes of different maximum depths: shallow (4 m), medium (13 m) and deep (24 m). Isotherm bands are in increments of 2 °C. Simulated water temperatures are for past climate (1955–79) (top) and the $2 \times CO_2$ GISS climate scenario (bottom).

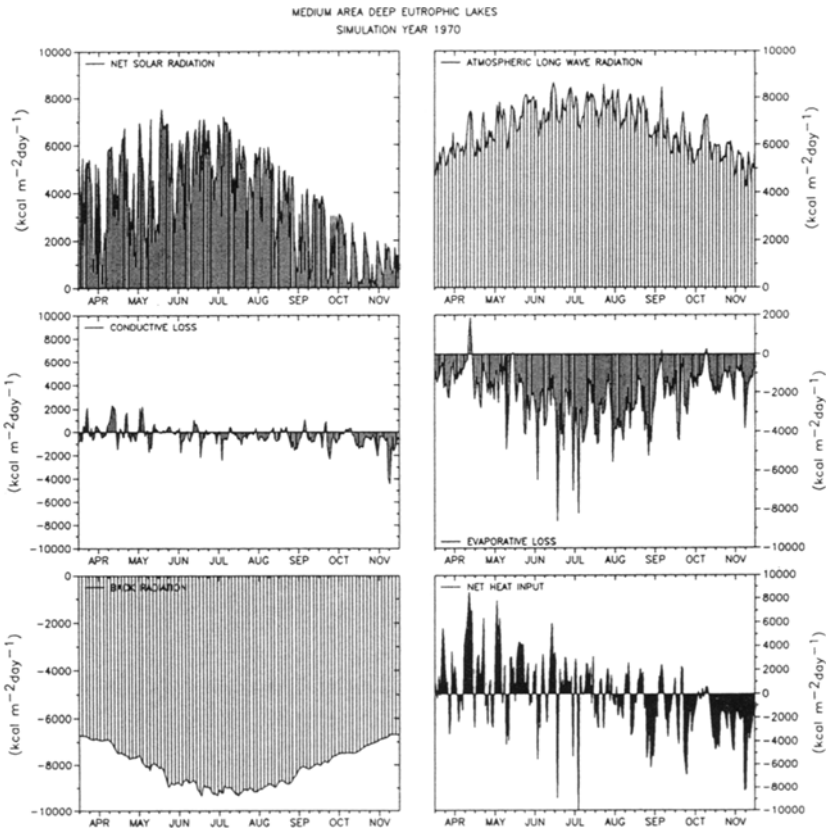

Fig. 9. Examples of individual surface heat flux components.

extraordinary dynamics and to explain them would take more space than available here, and may not be particularly fruitful.

Simulated cumulative net heat fluxes through the water surface are plotted in Figure 10 for past and future (GISS) climate conditions. The difference between the two is also shown in Figure 10. Lakes with large surface areas will receive more net heat input (up to 30%) than smaller ones, and in extremely small lakes the difference is even negative, meaning less heat will be transferred through the water surface and stored in the lake! All net heat fluxes are per unit surface area of a lake, not total values.

Back radiation and evaporation are the main processes by which lakes lose heat in the summer. Evaporative losses were found to be significantly increased after climate change (GISS). This is due to higher vapor pressure at the water surface despite decreased wind speeds during midsummer. In all lakes, regardless of depth, surface area and trophic status, the computed evaporation water losses were uniformly 0.30 m ($\pm$ 0.01 m) higher (Figure 11). In other words, lake water budgets will be put under significant stress. This increased evaporation also explains why

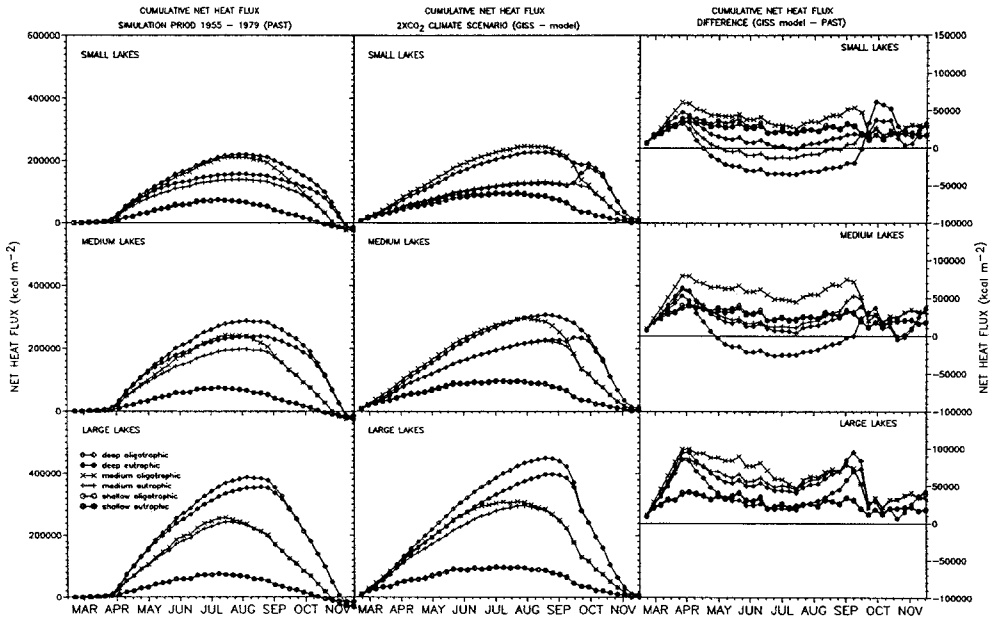

Fig. 10. Simulated cumulative net heat flux.

the water temperature increases after climate change remains at a relatively moderate 2 °C, when air temperature increases by an average seasonal simulation (March 1–November 30) value of 4.4 °C. Evaporative cooling is a key to the understanding of the temperature responses to changed climate. The additional evaporation is in response to increased heat input from the atmosphere. The net increase in heat input to the surface layer is still positive but kept lower by increased evaporative water losses. The effect on surface stratification stability and mixing is handled by the turbulent heat transfer equation and the wind mixing algorithm.

5.3. *Vertical Mixing/Stratification/Stability*

Vertical mixing and stratification affect lake water temperature dynamics. A surface mixed layer depth is defined here as the thickness of the isothermal layer from the water surface downward. Surface mixed layer depths are calculated daily by the wind mixing algorithm in the model and averaged over a week (Figure 12). Mixed layer depths at the beginning and before the end of simulation are equal to the total lake depth and indicate spring and fall overturns. The most shallow mixed layer depths were calculated for small, deep, eutrophic lakes based on the classification in Table II. Vertical mixing is caused by wind and natural convection. Surface mixed

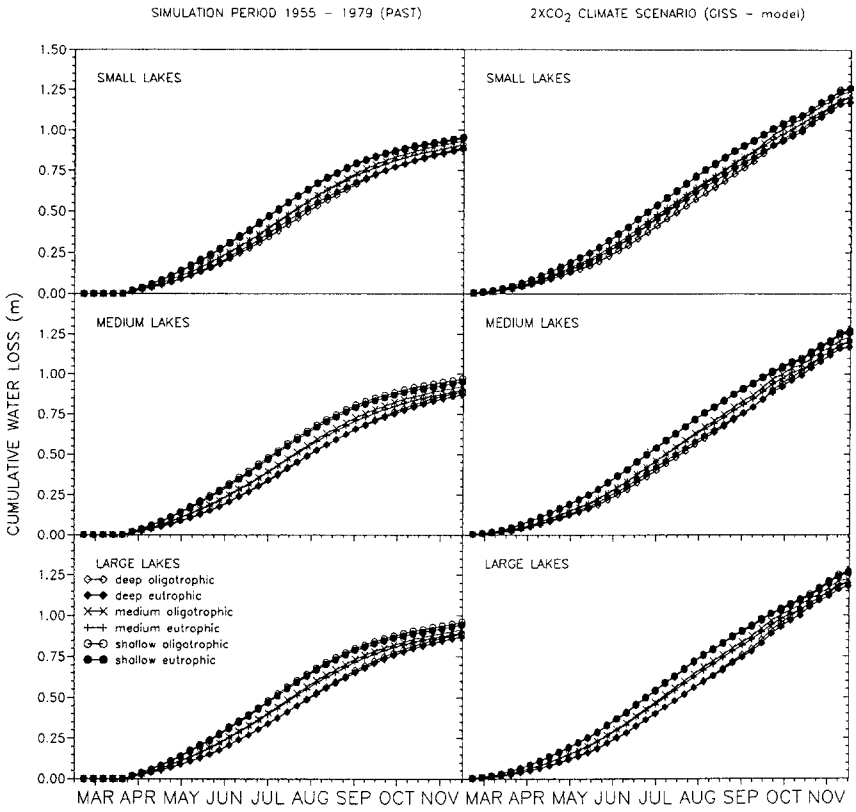

Fig. 11. Simulated cumulative evaporative losses.

layer depths were the shallowest for small lakes because of short fetch. Smaller wind stressed and hence wind energy inputs are usually associated with smaller lake surface area (shorter fetch). In these lakes the smallest amount of turbulent kinetic energy is available for entrainment of the thermocline. Wind energy required for entrainment of layers at the thermocline is proportional to the stability (defined as a density difference between adjacent layers) of the water column and depth of the mixed layer. The lowest hypolimnetic temperatures and the highest temperature (density) gradients were calculated for small, deep, eutrophic lakes. That was the reason for the smallest mixed layer depths calculated for these lakes.

For the same morphometric lake characteristics, oligotrophic lakes had deeper surface mixed layers than eutrophic lakes because of higher penetration depth of irradiance.

Climate change will impose higher positive net heat fluxes at the lake surface earlier in the season than in the past. That causes an earlier onset of stratification. This is in agreement with a conclusion derived by Robertson (1989) from field data for Lake Mendota. In the period from the onset of stratification until September, mixed layer depths were projected in the average 1.2 m smaller than in the past.

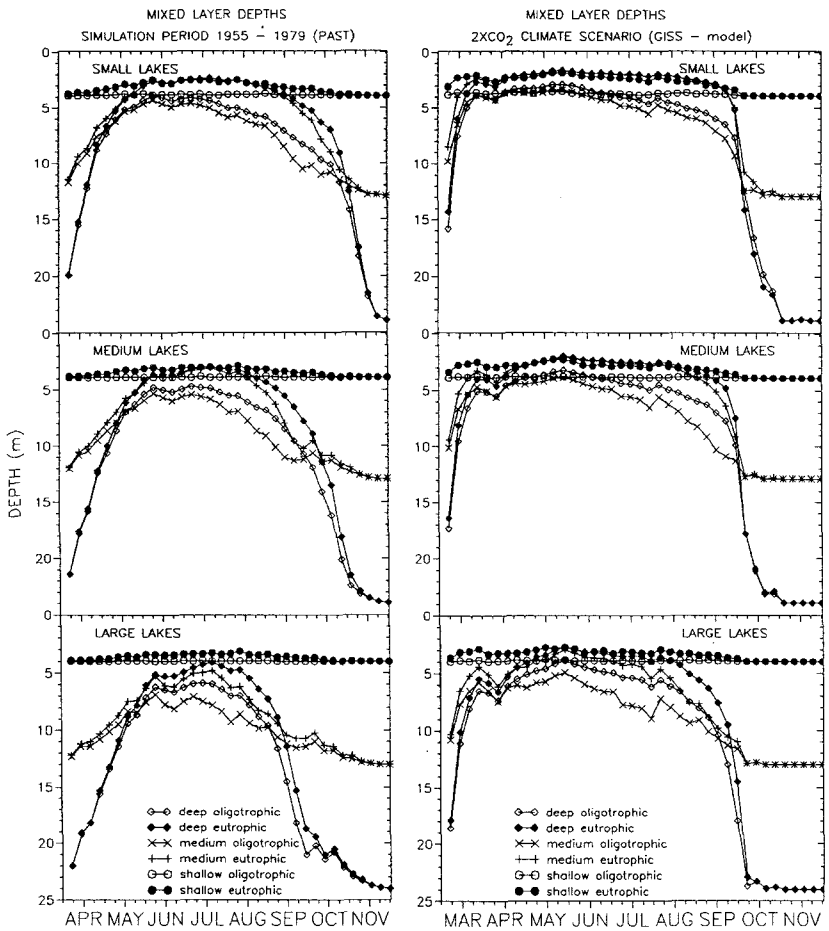

Fig. 12. Simulated weekly mixed layer depth.

From the end of September, mixed layer depths were deeper after climate change, mainly due to stronger natural convection and higher winds caused by climate change. In spring and summer evaporative losses were also increased by climate change but no significant persistent cooling occurred because of net heat input from radiation and convection. The earlier onset of stratification in spring and the mixed layer depth increase in fall were also found by Schindler *et al.* (1990) in his analysis of observations in the Experimental Lakes Area (ELA). Mixed layer depths increased due to transparency increase and increased winds due to reduced forest cover resulting from increased incidence of forest fires.

The stabilizing effect of the density stratification and the destabilizing effect of the wind can be quantified using a Lake number (Imberger and Patterson, 1989):

$$L_n = \frac{g S_t (1 - z_t/z_m)}{\rho_0 u_* A_0^{3/2} (1 - z_g/z_m)} \tag{2}$$

where g is acceleration due to gravity (m s^{-2}), z_t is height from the lake bottom to the center of the thermocline (m), z_m is maximum lake depth (m), z_g is the height of the center of volume of lake, A_0 is lake surface area (m^2), ρ_0 is hypolimnion density (kg m^{-3}), S_t is the stability of the lake (kg m; Hutchinson, 1957), u_* is surface shear velocity (m s^{-1}). Estimates for the different elements in the Lake number are obtained from daily lake water temperatures simulations, daily meteorological data, and lake geometry. Larger Lake number values indicate stronger stratification and higher stability i.e. forces introduced by the wind stress will have minor effect. Lake number dependence on lake area, depth, and trophic status, for different lake classes is given in Figure 13. Stability is higher for oligotrophic lakes than eutrophic lakes. Oligotrophic lakes had deeper thermoclines and required greater wind force in order to overturn the density structure of the water column. Climatic change caused higher lake numbers, i.e. more stable stratification among the same lake classes.

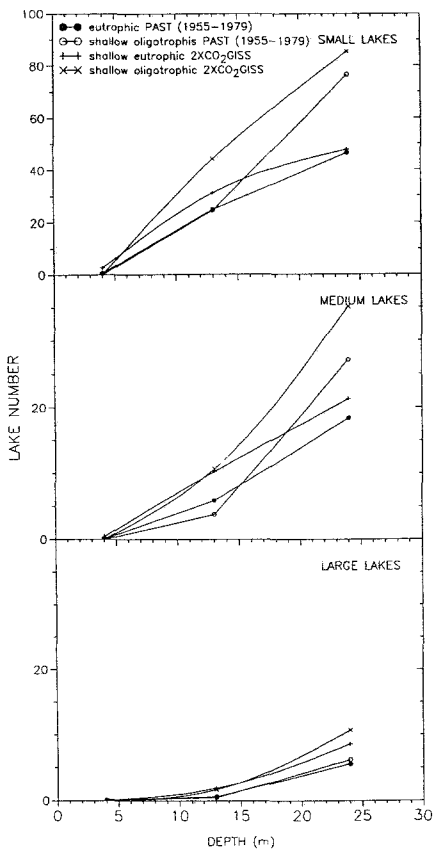

Fig. 13. Simulated lake numbers as a function of lake depth and trophic status.

Climate change advanced the onset of seasonal stratification in the average by 50 days for shallow lakes, and 34 days for deep and medium deep lakes. Length of stratification was prolonged by 60 days for shallow and by 40 days for deep and medium deep lakes.

6. Conclusions

A regional simulation study was conducted for 27 classes of lakes in Minnesota. Lakes were classified according to area, maximum depth, and trophic level. A validated, one-dimensional, unsteady lake water quality model was linked to global climate model output in order to quantify potential thermal changes in inland lakes due to climate change. Water temperatures were simulated on a daily time base for past weather conditions, 1955–1979 and the $2 \times CO_2$ GISS model climate scenario.

The main findings are as follows:

(a) Simulated epilimnetic temperatures were predominantly related to weather and secondarily to lake morphometry. Weekly average epilimnetic temperatures were raised by climate change for all lake classes. The seasonally averaged water temperature rise was 3 °C, compared to 4.4 °C air temperature increase caused by the climate change. The largest differences in water temperatures occurred in April and September, and were 7.2 and 4.9 °C. The seasonal daily maximum of epilimnetic temperatures rose only about 2 °C with climate change.

(b) Hypolimnetic temperatures were predominantly related to lake morphometry and mixing events in spring, and only secondarily to weather in summer. The highest temperatures were calculated for large, shallow, eutrophic lakes. After climate change, hypolimnetic water temperatures were as follows: shallow lakes, warmer by an average 3.1 °C; deep lakes, cooler by an average 1.1 °C; small area, medium depth lakes, cooler by 1.7 °C; and large-area medium-depth lakes, warmer by 2.0 °C. The cooler temperatures are caused by an onset of seasonal stratification at lower well-mixed lake water temperatures earlier in the season due to higher net heating rates after climate change.

(c) Simulated evaporative heat and water losses increased by about 30% for the $2 \times CO_2$ GISS climate scenario. Evaporative water losses increased by about 300 mm, making the total water loss 1200 mm.

(d) Net heat flux at the lake surface increased with changed climatic conditions. The largest difference in calculated cumulative net heat storage between past and future climate was 100,000 kcal m^{-2} and occurred in April and September with climate change.

(e) Simulated mixed layer depths decreased about 1 m in the spring and summer, and increased in the fall.

(f) With climate change, lakes stratify earlier, and overturned later in the season. Length of the stratification period was increased by 40 to 60 days.

(g) Climate change caused greater lake stability in spring and summer. In fall lakes were driven faster towards isothermal conditions.

Acknowledgement

The investigation described herein was conducted for the U.S. Environmental Protection Agency/OPPE in cooperation with the Environmental Research Laboratory Duluth as part of a project on climate change effects on fisheries. The project officer was J. G. Eaton. Other cooperating staff members were B. Goodno, K. Hokanson, and H. McCormick. Project No. CR-816230-01-0.

Mr. Dennis Schupp, Minnesota Department of Natural Resources, Fisheries Division, provided the original lake data (MFLD database) from which the frequency distributions of surface areas, depth and Secchi depth were derived.

The Minnesota Supercomputer Institute, University of Minnesota, provided a resource grant and access to its CRAY 2 supercomputer.

References

Baker, D. G., Kuehnast, E. L., and Zandlo, J. A.: 1985, 'Climate of Minnesota, Part 15 – Normal Temperatures (1951–1980) and Their Application', Agricultural Experimental Station University of Minnesota, AD-SB-2777.

Blumberg, A. F. and Di Toro, D. M.: 1990, 'Effects of Climate Warming on Dissolved Oxygen Concentrations in Lake Erie', *Transact. Amer. Fisher. Soc.* **119(2)**, 210–223.

Carlson, R. E.: 1977, 'A Trophic State Index for Lakes', *Limnol. Oceanogr.* **22**, 361–369.

Coutant, C. C.: 1990, 'Temperature-Oxygen Habitat for Freshwater and Coastal Striped Bass in a Changing Climate', *Transact. Amer. Fish. Soc.* **119(2)**, 240–253.

Croley II, T. E.: 1990, 'Laurentian Great Lakes Double-CO_2 Climate Change Hydrological Impacts', *Clim. Change* **17**, 27–47.

ERLD/MNDNR: 1990, 'Minnesota Department of Natural Resources Fisheries Division Lake Data Base', expanded by U.S. Environmental Protection Agency Environmental Research Laboratory Duluth.

Ford, D. E. and Stefan, H. G.: 1980, 'Thermal Predictions Using Integral Energy Model', *Jour. Hydraul. Divis. ASCE* **106**, HY1, 39–55.

Gorham, E. and Boyce, F. M.: 1989, 'Influence of Lake Surface Area and Depth upon Thermal Stratification and the Depth of the Summer Thermocline', *J. Great Lakes Res.* **15**, 233–245.

Gu, R. and Stefan, H. G.: 1990, 'Year-Round Temperature Simulation of Cold Climate Lakes', *Cold Regions Sci. Technol.* **18**, 1–14.

Heiskary, S. A., Wilson, C. B., and Larsen, D. P.: 1987, 'Analysis of Regional Patterns in Lake Water Quality: Using Ecoregions for Lake Management in Minnesota', *Lake Reserv. Manag.* **3**, 337–344.

Heiskary, S. A. and Wilson, C. B.: 1988, 'Minnesota Lake Water Quality Assessment Report', Minnesota Pollution Control Agency, St. Paul, p. 49.

Henderson-Sellers, B.: 1988, 'Sensitivity of Thermal Stratification Models to Changing Boundary Conditions', *Appl. Mathemat. Modell.* **12**, 31–43.

Hengeveld, H. G.: 1990, 'Global Climate Change: Implications for Air Temperature and Water Supply in Canada', *Transact. Amer. Fisher. Soc.* **119(2)**, 176–182.

Hondzo, M. and Stefan, H. G.: 1991, 'Three Case Studies of Lake Temperature and Stratification Response to Warmer Climate', *Water Resourc. Res.* **27(8)**, 1837–1846.

Hondzo, M. and Stefan, H. G.: 1992a, 'Propagation of Uncertainty due to Variable Meteorological Forcing in Lake Temperature Models', *Water Resourc Res.* **28(10)**, 2629–2638.

Hondzo, M. and Stefan, H. G.: 1992b, 'Water Temperature Characteristics of Lakes Subjected to Climate Change', University of Minnesota, St. Anthony Falls Hydraulic Laboratory, Project Report No. 329, p. 185, August.

Hutcinson, G. E.: 1957, 'A Treatise on Limnology', Vol. I, John Wiley & Sons, Inc., p. 1015.

Imberger, J. and Patterson, J. C.: 1989, 'Physical Limnology', in Hutchinson, J. W. and Wu, T. Y. (eds.), *Advances in Applied Mechanics*, Academic Press, Vol. **27**, 303–475.

Jones, P. D., Wigley, T. M. L., and Wright, P. B.: 1986, 'Global Temperature Variations between 1861 and 1984', *Nature* **332(31)**, 430–434.

Kerr, R. A.: 1989, '1988 Ties for Warmest Year', *Science* **243(17)**, 891–892.

Magnuson, J. J., Meisner, J. D., and Hill, D. K.: 1990, 'Potential Changes in Thermal Habitat of Great Lakes Fish After Global Climate Warming', *Transact. Amer. Fisher. Soc.* **119(2)**, 254–264.

McCormick, M. J.: 1990, 'Potential Changes in Thermal Structure and Cycle of Lake Michigan Due to Global Warming', *Transact. Amer. Fisher. Soc.* **119(2)**, 183–194.

Meisner, J. D., Goddier, J. L., Regier, H. A., Shuter, B. J., and Christie, W. J.: 1987, 'An Assessment of the Effects of Climate Warming on Great Lakes Basin Fishes', *J. Great Lakes Res.* **13(3)**, 340–352.

National Center for Atmospheric Research: 1990, Data Support Section, Personal communication Roy Jenne and Dennis Joseph, Boulder, Colorado.

Omernick, J. M.: 1987, 'Ecoregions of the Conterminous United States', Annals of the Assoc. of Amer. Geogr. Vol. **77(1)**, 118–125.

Riley, M. J. and Stefan, H. G.: 1988, 'MINLAKE: A Dynamic Lake Water Quality Simulation Model', *Ecolog. Modell.* **43**, Elsevier Science Publ., Amsterdam, 155–182.

Robertson, D. M.: 1989, 'The Use of Lake Water Temperature and Ice Cover as Climatic Indicators', Ph.D. thesis, University of Wisconsin-Madison, p. 330.

Robinson, P. J. and Finkelstein, P. L.: 1990, 'Strategies for the Development of Climate Scenarios for Impact Assessment: Phase I Final Report', USEPA, Atmospheric Research and Exposure Assessment Laboratory, EPA/600/53-90/026.

Schertzer, W. M. and Sawchuk, A. M.: 1990, 'Thermal Structure of the Lower Great Lakes in a Warm Year: Implications for the Occurrence of Hypolimnion Anoxia', *Transact. Amer. Fisher. Soc.* **119(2)**, 195–209.

Schindler, D. W., Beaty, K. G., Fee, E. J., Cruikshank, D. R., DeBruyn, E. R., Findley, D. L., Londsey, G. A., Sherer, J. A., Stainton, M., and Turner, M. A.: 1990, 'Effects of Climatic Warming on Lakes of the Central Boreal Forest', *Science* **250**, 16 November, 967–970.

Stefan, H. G.: 1989, 'Lake Mixing Dynamics and Water Quality Models', *J. Minnes. Acad. Sci.* **55**, No. 1.

Stefan, H. G. and Ford, D. E.: 1975, 'Temperature Dynamics in Dimictic Lakes', *J. Hydraul. Divis. ASCE* **101**, No. HY1, 97–114.

Stefan, H. G., Hanson, M. J., Ford, D. E., and Dhamotharan, S.: 1980, 'Stratification and Water Quality Predictions in Shallow Lakes and Reservoirs', Proc. Second Int'l Symp. on Stratified Flows, International Association for Hydraulic Research, 1033–1043.

(Received 13 April 1992; in revised form 20 November 1992)